J. Fluid Mech. (1972), *vol.* 55, *part* 2, *pp.* 209–227
Printed in Great Britain

Mixed convection over a heated horizontal plane

By A. A. TOWNSEND
Emmanuel College, Cambridge

(Received 3 January 1972 and in revised form 19 June 1972)

Measurements of velocity and temperature fluctuations have been made in flows of air over a strongly heated horizontal surface in conditions of large negative Richardson number and approximating to horizontally homogeneous turbulent flow with constant shear stress and upwards flux of total heat. Within a layer that includes most of the total variation of mean temperature and velocity, the effect of the mean flow on the thermal structure is nearly confined to a change in the length scale which measures the thickness of the viscous–convective layer at the surface but which is also the length scale for the fully turbulent region. Measurements of the mean velocity and the mean-square fluctuation in the stream direction were made for a flow velocity of about $0{\cdot}70\,\mathrm{m\,s^{-1}}$ and showed that the profiles of mean temperature and mean velocity are closely similar, implying proportionality at each height of the transfer coefficients for heat and for momentum. The ratio is estimated to be $1{\cdot}4$. The measurements were carried out in conditions such that the Monin–Obukhov length was in the range 8–60 mm and the maximum height of observation was 80 mm.

1. Introduction

Convective transfer of sensible heat through the earth's boundary layer has a large effect on the motion there, and several studies of the velocity and temperature fields have been made over terrain sufficiently uniform for the flow to be nearly homogeneous over horizontal planes (e.g. Dyer 1967). In these conditions, the Reynolds stress and vertical heat flux are nearly independent of height, and dimensional analysis shows that suitably defined non-dimensional velocity and temperature gradients depend only on the ratio of the height to the Monin–Obukhov length, determined by the buoyancy flux and the shear stress. For large values of the ratio, buoyancy forces are dominant and the flow should resemble natural convection over a horizontal plane with the same heat transfer. For small values, the buoyancy forces are relatively small and the flow is one of forced convection with motion independent of the heat transfer. The present work was undertaken as an attempt to discover some of the details of the flow in the intermediate region between the forced convection near the surface and the natural convection far above it.

Field studies and laboratory measurements of convective flows each have their difficulties and advantages. As will be seen, an acceptable degree of horizontal homogeneity could be attained only in conditions of zero wind or in conditions of less than extreme instability, but it was possible to measure profiles of mean

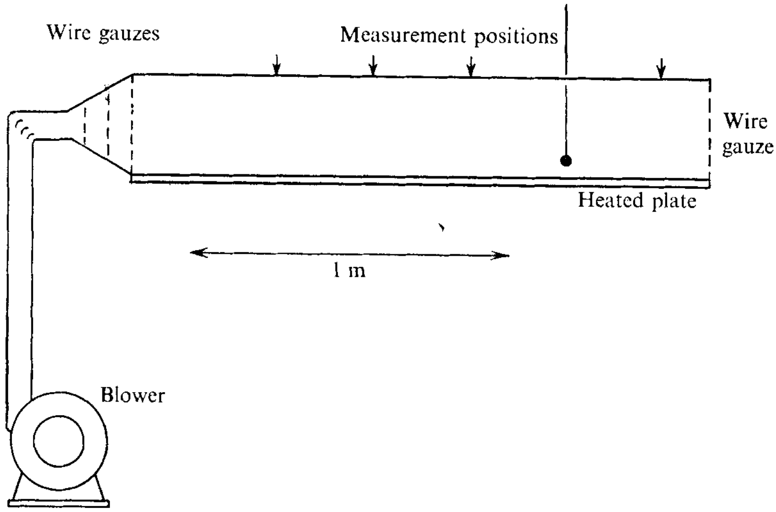

FIGURE 1. Sketch of vertical section of the convection duct.

values and intensities of fluctuation for velocity and temperature. The measurements covered a range of Richardson numbers between $-0\cdot1$ and about -5 in the region of fully turbulent flow; this is very nearly the same range as that for the observations in the atmosphere.

2. Experimental details

The flows were set up in a duct of square cross-section, shown diagrammatically in figure 1. The inside width of the duct was 305 mm and it was 1·83 m long. The bottom was a dural plate 12·7 mm thick and electrically heated to a temperature that was uniform to within a few tenths of a degree for a temperature rise of 40 °K. The sides were of hardboard and the top was a dural plate 4·8 mm thick. A controlled flow of air was obtained from a centrifugal blower driven by a synchronous motor. The air passed through a gauze-filled expansion chamber before entering the duct, and the exit to the room was covered with wire gauze to exclude draughts.

Measurements of temperature were made with resistance thermometers of Wollaston wire, 2·5 μm in diameter and about 2 mm long, using the electronic equipment for analysis and averaging described in an earlier paper (Townsend 1959*b*). Measurements of mass flow in the stream direction and of its fluctuation were made with an anemometer essentially similar to that developed by Taylor (1958) for use in the atmosphere. It consists of two parallel temperature-sensitive wires (of tungsten, 0·025 mm diameter, about 10 mm long and 1·5–2 mm apart), with a heated wire (of nichrome, 0·04 mm diameter) between them and at right angles to the plane of the parallel wires. The temperature-sensitive wires were connected in a bridge which was balanced for equal temperatures of the wires. The bridge was supplied from a 10 kHz oscillator whose amplitude was controlled to maintain a constant level of bridge output. With the heated wire supplying heat at a constant rate to the flow, the oscillator output is expected to be proportional to the component of mass flow in the direction at right angles to all three wires, provided that the flow velocity is not so small that heat is transferred to the upstream thermometer wire by conduction. For the configuration used, the limit was about $0{\cdot}08\,\mathrm{m\,s^{-1}}$. The instrument was calibrated in a wind tunnel over a speed range of about $0{\cdot}3$–$5\,\mathrm{m\,s^{-1}}$, the primary measurement being the time-of-flight of temperature variations introduced into the flow. It has the considerable advantage of being relatively little affected by fluctuations of temperature and of a linear response to a single component of mass flow. Mean values and fluctuation intensities were measured with the same equipment; all the measured values are averages over periods of at least 10 min.

The object was to obtain fully developed turbulent flow towards the end of the duct so that conditions in the bottom 80 mm might approximate to the ideal conditions of Reynolds stress and heat flux independent of height. For all conditions, the heating of the bottom plate was sufficiently strong for convective turbulent flow to be established over the whole section of the duct within one metre of the entrance, but the heating of the cold air entering the duct produced large horizontal gradients of temperature near the entrance. The consequence is that the flow near the surface is accelerated in the same way as a sea breeze and, particularly at the lower wind speeds, flows resembling wall jets with strong maxima in their velocity profiles are found. In figure 2, profiles of mean velocity are shown for a general flow velocity of about $0{\cdot}2\,\mathrm{m\,s^{-1}}$ and surface temperature 31 °K above the temperature near the centre of the duct. It will be seen that the velocity peak half-way along the duct is 1·75 times the general velocity of flow and that the maximum is still obvious at the exit. Fortunately, the effect is much less for flow velocities of $0{\cdot}65\,\mathrm{m\,s^{-1}}$ and above and, at stations 5 and 6 (respectively 1·37 m and 1·68 m from the entrance), the profiles of both velocity and temperature are nearly identical and the flow is nearly fully developed.

3. Notation and non-dimensional representation of results

The flow is described using a co-ordinate system with origin at the upstream edge of the working section, Ox being in the direction of flow and Oz vertically upwards. Parallel mean flow is assumed and the components of velocity are $U+u$, v and w, where U is the time-averaged value. The local temperature is $T+\theta$ (°K). To the extent that the experimental flows are horizontally homogeneous, they are specified by U_a, the mean velocity near the duct centre, by T_1, the surface temperature, and by the mean temperature T_a near the centre.

The measurements have been reduced and presented on the assumption that the temperature differences are small enough to permit use of the Boussinesq approximation – that density variations may be ignored except in so far as they lead to buoyancy forces on the fluid – and that the shear stress τ_0 and the upward flux H of total heat are independent of height above the surface. The temperature differences do lead to noticeable variations of density but, as Thomas & Townsend (1957) have shown, the effect of finite differences on heat-transfer relations can be removed by using natural logarithms of temperature ratios in place of differences.

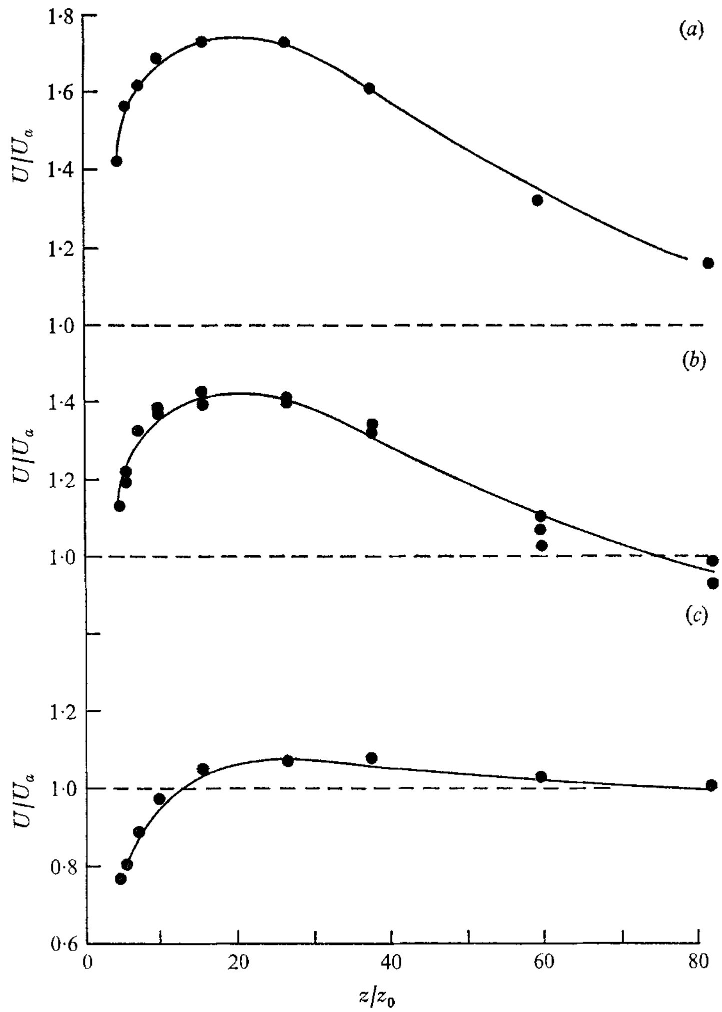

FIGURE 2. Mean velocity profiles for $T_1 - T_a = 31$ °C and $U_a = 200$ mm s^{-1}. (a) $x = 1{\cdot}06$ m. (b) $x = 1{\cdot}37$ m. (c) $x = 1{\cdot}68$ m.

The equations of motion and heat in the Boussinesq approximation may be put into non-dimensional form by using the natural scales of velocity, length and logarithm of absolute temperature:

$$u_0 = (\kappa g Q)^{\frac{1}{4}}, \quad z_0 = \kappa^{\frac{3}{4}}(gQ)^{-\frac{1}{4}}, \quad \theta_0 = Q^{\frac{3}{4}}(\kappa g)^{-\frac{1}{4}}, \tag{3.1†}$$

where κ is the thermometric conductivity of the fluid and $Q = H/\rho c_p T$ is the thermometric heat flux. If the flow is independent of distant boundaries, the boundary conditions are specified by $\log T_a$, τ_0 and gQ, and the non-dimensional coefficients in the equations can be expressed in terms of the Prandtl number ν/κ and the ratio of the Monin–Obukhov length $L = \tau_0^{\frac{3}{2}}(\kappa g Q)^{-1}$ to the thermal scale z_0.

† The thermal length scale z_0 should not be confused with the roughness length.

It follows that the distributions of mean velocity and mean temperature have the functional forms

$$\left.\begin{aligned} U &= u_0 f(z/z_0, L/z_0, \nu/\kappa), \\ \log(T/T_a) &= \theta_0\, g(z/z_0, L/z_0, \nu/\kappa), \end{aligned}\right\} \tag{3.2}$$

and in particular that

$$\left.\begin{aligned} \log(T_1/T_a) &= \theta_0\, g(0, L/z_0, \nu/\kappa), \\ U_a &= u_0 f(\infty, L/z_0, \nu/\kappa). \end{aligned}\right\} \tag{3.3}$$

In the experiments, the shear stress could be estimated only in favourable circumstances and the determination of heat flux was not very accurate. It seemed preferable to substitute for θ_0 and u_0 the related scales

$$\theta_1 = \log(T_1/T_a), \quad u_1 = (\kappa g \theta_1)^{\frac{1}{3}}. \tag{3.4}$$

Using the relations (3.2) and (3.3) shows that the mean profiles should have the forms

$$\left.\begin{aligned} U &= u_1 F(z/z_0, L/z_0, \nu/\kappa), \\ \log(T/T_a) &= \theta_1 G(z/z_0, L/z_0, \nu/\kappa). \end{aligned}\right\} \tag{3.5}$$

In practice, the values of $\log(T_1/T)$ and U at $z = 76$ mm were used as adequate approximations to θ_1 and U_a. In the absence of measurements of shear stress, the parameter L/z_0 cannot be used and it is replaced by U_a/u_1, which depends only on L/z_0 and the Prandtl number.

4. Heat-transfer coefficients

For natural convection above a heated horizontal plane in air (Prandtl number $= 0{\cdot}77$), the heat-transfer relation can be expressed in the form

$$Q = C(\kappa g)^{\frac{1}{3}}[\log(T_1/T_a)]^{\frac{4}{3}}, \tag{4.1}$$

where $C = 0{\cdot}18$ (see Thomas & Townsend 1957) is a heat-transfer coefficient. Equation (3.5) of the previous section implies that

$$C' = Q/(\kappa g)^{\frac{1}{3}}[\log(T_1/T_a)]^{\frac{4}{3}} = fn(U_a/u_1), \tag{4.2}$$

and C' can be calculated from any set of temperature measurements that lies well within the viscous–conductive layer. In that layer the root-mean-square temperature fluctuation is proportional to the distance from the surface and temperature is a linear function of distance, so that the surface temperature and surface temperature gradient may be found by extrapolating to the position of zero fluctuations. The procedure was used to calculate the heat-transfer coefficient from all the suitable runs, details of which are to be found in table 1; figure 3 shows the values of C' as a function of the flow parameter U_a/u_1. Within the experimental error, the results may be represented by

$$C' = 0{\cdot}20(1 + 0{\cdot}025 U_a/u_1) \tag{4.3}$$

over the range $0 \leqslant U_a/u_1 \leqslant 31$. (The discrepancy between the value of $U_a/u_1 = 0$ and the value of C found by Thomas & Townsend is mostly a consequence of defining T_a as the temperature at $z = 76$ mm.)

Run	x	$\log(T_1/T_a)$	U_a	Q	C'	z_0	U_a/u_1	$\dfrac{(\overline{\theta^2})^{\frac{1}{2}}_{\max}}{T\log(T_1/T_a)}$
A 1	0·46 m	121×10^{-3}	97	0·71	0·24	1·03	3·5	0·25
A 2	1·07	123	97	0·67	0·19	1·04	3·3	0·20
A 3	1·07	136	322	0·71	0·17	1·03	10·7	0·174
A 4	1·07	139	322	0·72	0·17	1·03	10·7	0·179
A 5	1·07	103	650	0·72	0·25	1·03	23·7	0·179
A 6*a*	1·07	103	650	0·90	0·31	0·97	23·7	0·182
A 6*b*	1·37	115	704	0·90	0·28	0·97	25·0	0·181
B 1	1·37	110	704	0·98	0·32	0·95	25·0	0·186
B 2	1·37	61·7	704	0·47	0·33	1·14	31·0	0·196
B 3	1·37	55·7	704	0·43	$0{\cdot}34_5$	1·17	31·0	0·208
B 4	1·07	60·5	704	0·54	0·39	1·10	31·0	0·186
B 5	1·37	112	704	1·10	0·35	0·92	25·0	0·198
B 6	1·37	127	361	1·07	$0{\cdot}28_5$	0·93	12·3	0·206

TABLE 1. Temperature runs. Note that the units of U_a and Q are mm s^{-1}; units of z_0 are mm.

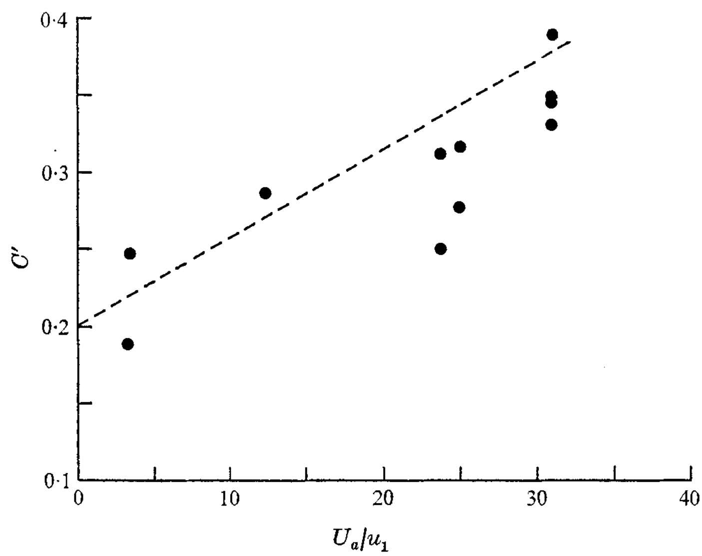

FIGURE 3. Non-dimensional heat-transfer coefficient as a function of the stability parameter U_a/u_1.

All the measurements refer to strongly unstable conditions, but there is some justification for the extrapolation of the linear variation (4.3) to very large values of U_a/u_1 representing conditions of forced convection. If the whole flow is one of forced convection, similarity arguments based on defect laws for the distributions of velocity and temperature in the fully turbulent flow lead to the result

$$C' = \frac{K_h}{K_m}\frac{\kappa^2}{[\log(\tau_0^{\frac{1}{2}}D/\nu)+C_m][\log(\tau_0^{\frac{1}{2}}D/\nu)+C_h]}\frac{U_a}{u_1}, \tag{4.4}$$

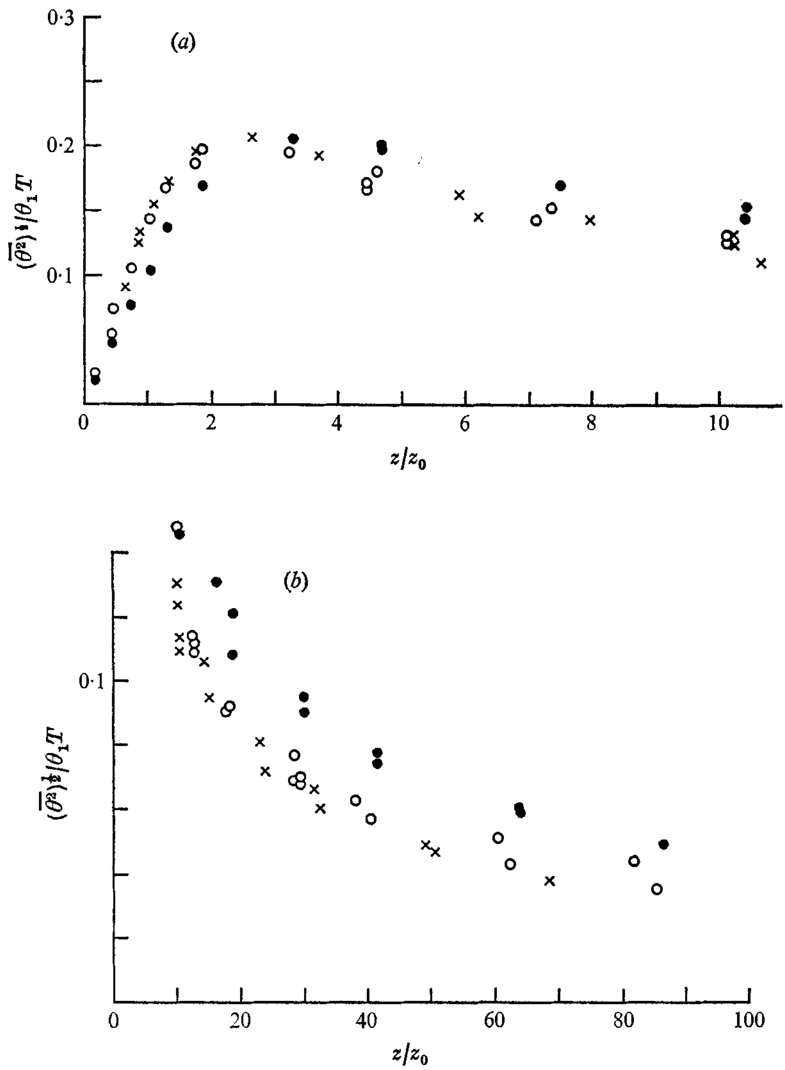

FIGURE 4. Intensities of temperature fluctuations as a function of height for various stability parameters. ●, run B6, $U_a/u_1 = 12{\cdot}3$; ○, runs B1 and B5, $U_a/u_1 = 25$; ×, runs B2 and B3, $U_a/u_1 = 31$. (*a*) Inner flow ($z/z_0 < 10$). (*b*) Outer flow.

where K_h/K_m is the ratio of the eddy diffusivity of heat to the eddy viscosity in a constant-stress layer, D is the half-width of the channel and C_m and C_h are flow constants defined by the similarity results

$$U_a = \frac{\tau_0^{\frac{1}{2}}}{\kappa}[\log(\tau_0^{\frac{1}{2}}D/\nu)+C_m],$$

$$\log(T_a/T_1) = -\frac{K_m}{K_h}\frac{Q}{\kappa\tau_0^{\frac{1}{2}}}[\log(\tau_0^{\frac{1}{2}}D/\nu)+C_h].$$

In (4.4), the coefficient of U_a/u_1 depends on the Reynolds number through the

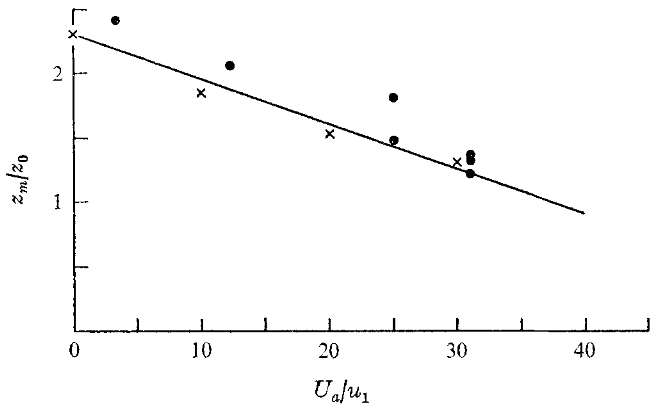

FIGURE 5. Variation of the thickness of the viscous–conductive layer with the stability parameter. ×, $C'(z_m/z_0)$ constant; ●, C' given by equation (4.3).

logarithmic factors but, if the Reynolds number is moderate, each factor is not far from seven and, if we suppose that $K_h/K_m = 1{\cdot}4$,

$$C' = 0{\cdot}005U_a/u_1$$

in agreement with equation (4.3) at large values of U_a/u_1.

5. Temperature profiles

In the viscous–conductive layer at the surface, momentum and heat are transferred mostly by molecular processes, and the mean velocity, mean temperature and root-mean-square temperature fluctuation vary linearly with distance from the surface. The thickness of the layer is, to some extent, set by considerations of its stability to disturbances introduced from the fully turbulent flow outside and it is expected to depend on both the heat transfer and the shear stress. From the measurements of temperature fluctuations (figures 4 and 6), it may be seen that the intensity reaches a maximum just outside the layer and a good and clear-cut measure of its thickness is the length

$$z_m = (\overline{\theta^2})^{\frac{1}{2}}_{\max}/(d(\overline{\theta^2})^{\frac{1}{2}}/dz), \tag{5.1}$$

where the denominator is evaluated for z/z_0 small.

Values of z_m determined in this way are plotted in figure 5 as fractions of z_0 against U_a/u_1, and a reasonable fit is obtained with

$$z_m/z_0 = 2{\cdot}3(1 - 0{\cdot}015U_a/u_1). \tag{5.2}$$

It is a more interesting fact that the product $C'(z_m/z_0)^{\frac{4}{3}}$ is, within the experimental scatter, constant over the range of U_a/u_1. The implication is that the variation of mean temperature over the viscous–conductive layer is the same fraction of the total variation in all conditions, and that profiles of mean temperature and intensity of temperature fluctuations can be correlated by using z_m as a length scale. Figure 6 shows the collapse of the measurements that is found for the

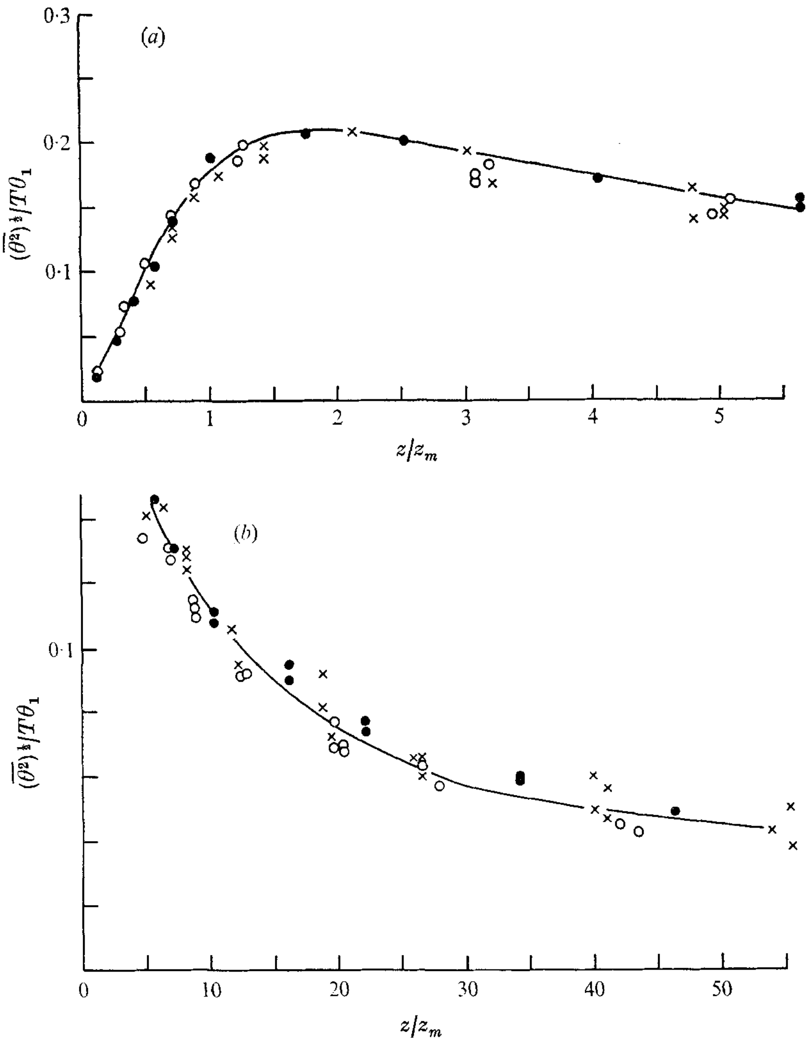

FIGURE 6. Non-dimensional intensities of temperature fluctuation as a ratio of the height to thickness of the viscous layer. ●, run B6, $z_m/z_0 = 1{\cdot}85$, $U_a/u_1 = 12{\cdot}3$; ○, runs B1 and B5, $z_m/z_0 = 1{\cdot}438$, $U_a/u_1 = 25$; ×, runs B2 and B3, $z_m/z_0 = 1{\cdot}230$, $U_a/u_1 \simeq 31$. (*a*) Inner flow ($z/z_0 < 10$). (*b*) Outer flow.

fluctuations and figure 7 shows the results for the mean temperatures. Because the air entering the duct is from the room and varies erratically in temperature, mean temperatures are less reproducible than intensities of fluctuations.

6. Velocity profiles

Measurements of mean velocity and velocity fluctuations were made in separate runs for three values of the flow parameter; table 2 gives details. For $U_a/u_1 = 25$, the sea-breeze caused by the entry conditions is not detectable beyond $x = 1{\cdot}2$ m and the measurements may be representative of the fully developed flow. In

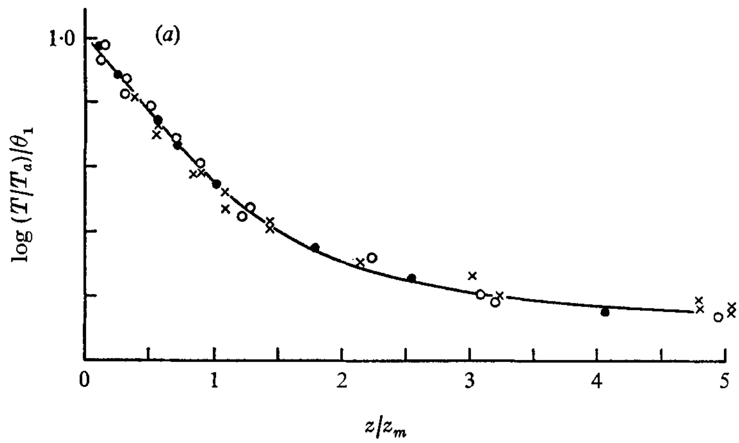

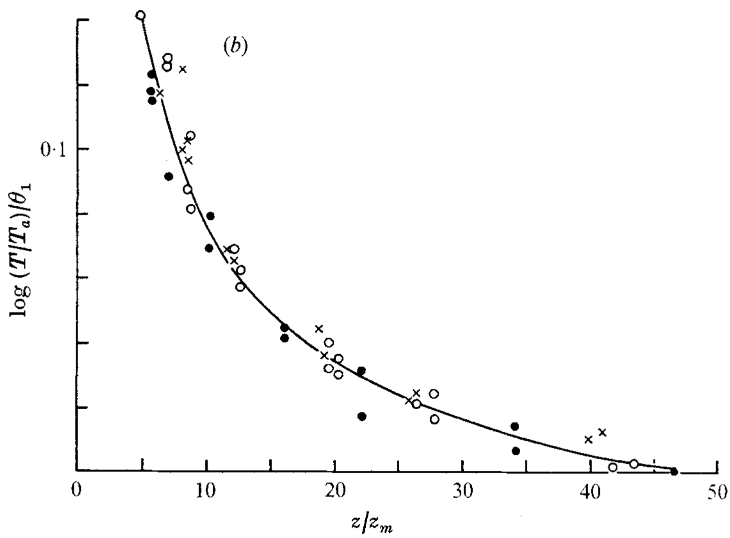

FIGURE 7. Non-dimensional mean temperature as a ratio of the height to thickness of the viscous layer. (*a*) Inner flow ($z/z_0 < 10$). (*b*) Outer flow. Notation as in figure 6.

Run	$10^3 \log(T_1/T_a)$	U_a	U_a/u_1	z_0 (mm)
D1	127	360	12·3	0·93
D2	127	200	6·0	0·92
D4	127	650	25·0	0·94
D4	127	700	25·0	0·94
D4	127	750	25·0	0·44

TABLE 2. Velocity runs. Note that the surface temperature ratio is an average over the temperature runs of table 1, i.e. A1, A2, A3, A4 and B6, and was not measured during the runs D1, D2 and D4.

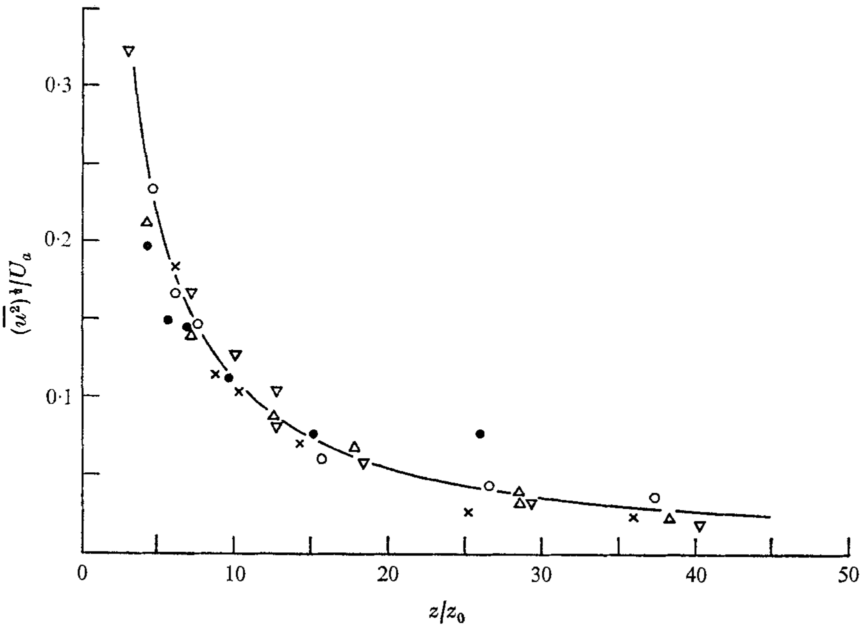

FIGURE 8. Similarity of mean velocity and mean temperature profiles for $U_a/u_1 = 25$. For $1 - U/U_a$, run D 4: ●, $x = 1{\cdot}06$ m; ○, $x = 1{\cdot}37$ m; ×, $x = 1{\cdot}68$ m. For $[\log(T/T_a)]/\theta_1$, $x = 1{\cdot}37$ m: △, run B 1; ▽, run B 5; ——, equation (6.1).

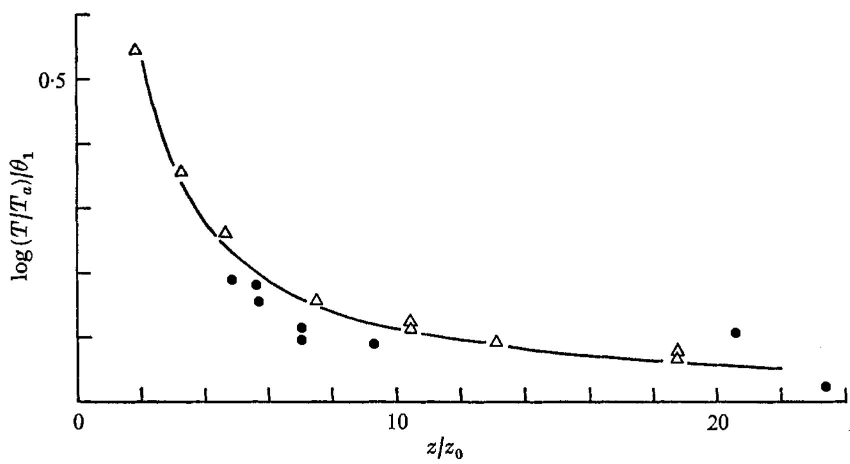

FIGURE 9. Similarity of mean velocity and mean temperature profiles for $U_a/u_1 = 12{\cdot}3$. ●, $1 - U/U_a$, run D 1; △, $\log(T/T_a)/\theta_1$, run B 6; ——, equation (6.1).

figure 8, values of the mean velocity at stations $1{\cdot}07$ m, $1{\cdot}37$ m and $1{\cdot}68$ m from the entrance are shown as velocity defect ratios $(1 - U/U_a)$ and are compared with measurements of mean temperatures for the same flow parameter. Over the range $5 \leqslant z/z_0 \leqslant 40$ the variations of velocity and temperature are remarkably similar, indicating a nearly constant ratio of the transport coefficients for heat and momentum. To provide a smooth curve, the following curve has been drawn:

$$1 - U/U_a = \log(T/T_a)/\log(T_1/T_a) = 1{\cdot}1 z_0/z, \tag{6.1}$$

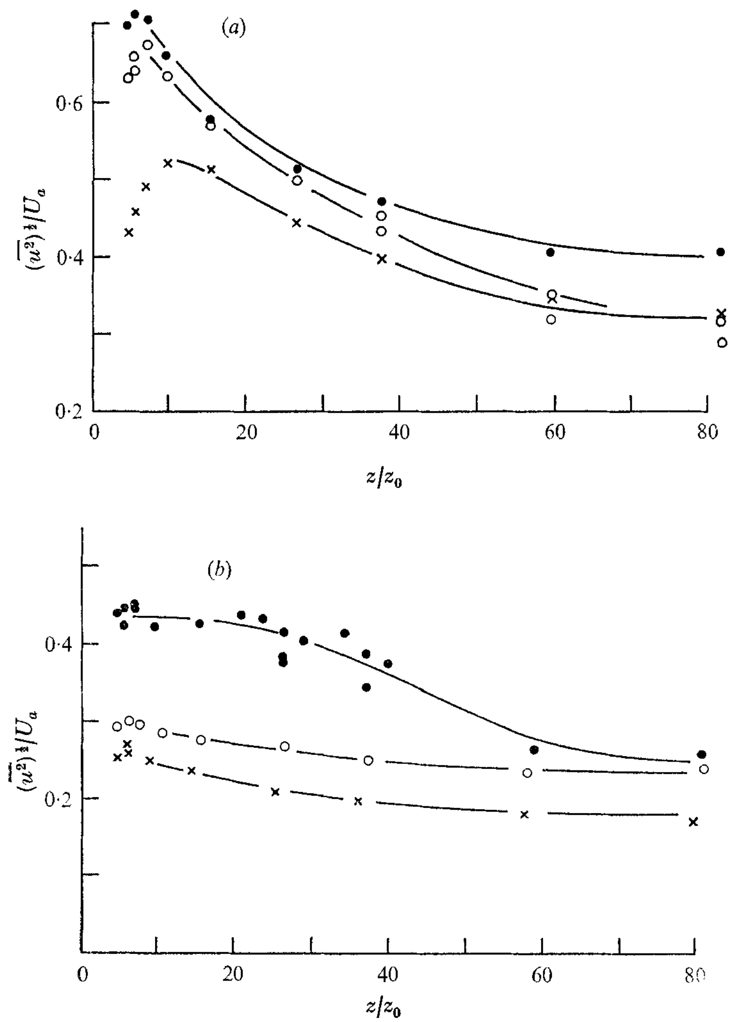

FIGURE 10. Variation with height of the root-mean-square velocity fluctuations. (a) Run D 2, $U_a/u_1 = 6$. ●, $x = 1{\cdot}06$ m; ○, $x = 1{\cdot}37$ m; ×, $x = 1{\cdot}68$ m. (b) ●, run D 1, $x = 1{\cdot}37$ m, $U_a/u_1 = 12{\cdot}3$; ○, run D 4, $x = 1{\cdot}37$ m, $U_a/u_1 = 25$; ×, run D 4, $x = 1{\cdot}68$ m, $U_a/u_1 = 25$.

but no significance need be attached to the exponent of z/z_0. By choosing other values for U_a and T_a, the observations could be described by power laws with exponents between $-0{\cdot}5$ and -1.

For $U_a/u_1 = 12{\cdot}3$ (see figure 9) initial conditions still have an effect on the velocity profile and the similarity with the temperature profile is less.

The intensity of the velocity fluctuations varies little over the range of heights (see figure 10); averaged values for $x = 1{\cdot}37$ m are listed in table 3. At the two lower speeds, the relative intensities are so large that reversal of the flow direction must be frequent, causing the measured intensities to exceed the true values. (Instead of decreasing to zero, the anemometer output becomes very large if the flow velocity falls below 20 mm s^{-1}.) It follows that the increase in the non-dimensional intensity $(\overline{u^2})^{\frac{1}{2}}/u_1$ with the flow parameter shown in the table is, if

Source	U_a/u_1	$(\overline{u_z^2})^{\frac{1}{2}}/u_1$	$(\overline{q^2})^{\frac{1}{2}}/u_1$	$(\overline{u^2})^{\frac{1}{2}}/U_a$
Townsend (1959*a*)	0	(2·3)	4	∞
Deardorff & Willis (1967)	0	2·2	3·5	∞
Run D 2	6	3·6	(6·2)	0·52
Run D 1	12·3	5·4	(9·4)	0·44
Run D 4	25·0	7·2–6·3	(10·9–12·5)	0·29–0·25

TABLE 3. Intensities of velocity fluctuations. Values in brackets assume that $\overline{q^2} = \overline{u^2}+\overline{v^2}+\overline{w^2} = 3\overline{u^2}$.

anything, less than the real increase, and the measurements are consistent with those with no mean flow reported by Townsend (1959*b*) and by Deardorff & Willis (1967). Within the considerable experimental uncertainty, the variation could be represented by a relation of the form

$$\frac{\overline{u^2}}{u_1^2} = \frac{(\overline{u^2})_0}{u_1^2}\frac{C'^2}{C_0^2} + \text{constant} \times C' \frac{U_a}{u_1^2} \tag{6.2}$$

(where the suffix 0 implies values for zero U_a/u_1), implying that the intensity is the sum of two components, one connected with heat transfer and one with momentum transfer.

The magnitude of the shear stress at the surface is an important quantity that cannot be measured directly. If equation (6.1) is used to approximate the distributions of velocity and temperature, the local Richardson number is given by

$$Ri = -0{\cdot}9(g\theta_1 z_0/U_a^2)\,(z/z_0)^2 \tag{6.3}$$

or, inserting the values for $U_a/u_1 = 25$,

$$Ri = -0{\cdot}0022(z/z_0)^2.$$

Near the inner limit of the velocity measurements, the Richardson number is calculated to be about $-0{\cdot}06$ and, if the turbulent flow there is hardly influenced by buoyancy forces, the neutral stability relation

$$\tau_0^{\frac{1}{2}} = kz\,dU/dz \tag{6.4}$$

can be used to estimate the shear stress. The friction velocity so found is $\tau_0^{\frac{1}{2}} = 63\,\text{mm}\,\text{s}^{-1}$ and the kinematic stress is $4000\,\text{mm}^2\,\text{s}^{-1}$, corresponding to a drag coefficient of $\tau_0/(\frac{1}{2}U_a^2) = 0{\cdot}016$. A large drag coefficient is expected since the viscous layer is much thinner than in an isothermal flow of the same speed. For example, the edge of the viscous layer is at the non-dimensional position $\tau_0^{\frac{1}{2}} z_m/\nu = 5$, and not near 12 as it would be in an isothermal flow.

Using the value of the surface stress, the Monin–Obukhov length is calculated to be

$$L = \tau_0^{\frac{3}{2}}/kgQ = 60\,\text{mm}$$

for flow with $U_a/u_1 = 25$. The parameter L/z_0 is 65, and most of the measurements for this flow condition are made at heights less than L. From the stress value, the ratio of the transport coefficients for heat and for momentum is found to be

$$\frac{K_h}{K_m} = \left(\frac{QT}{z\,dT/dz}\right)\Big/\left(\frac{\tau_0}{dU/dz}\right) = 1{\cdot}4 \pm 0{\cdot}2$$

for heights in the range $5 < z/z_0 < 30$.

7. Discussion

The comparatively accurate and consistent measurements of mean and fluctuating temperatures show that the mean flow has very little effect on the shapes of the profiles. The differences are in the characteristic scales of temperature variation and of length, $\theta_1 = \log(T_1/T_a)$ and z_m. If the similarity is exact, the flux of density defect is

$$Q = \text{constant} \times \kappa\theta_1/z_m$$

for all flow parameters and comparison with (4.2), defining the heat-transfer coefficient, leads to

$$C'(z_m/z_0)^{\frac{4}{3}} = \text{constant}, \tag{7.1}$$

in near agreement with measurements. It appears that the length scale of the convection is set by the thickness of the viscous–conductive layer and that the temperature structure is insensitive to the relative magnitudes of the inertial and buoyancy forces acting on the flow. On the other hand, the magnitude of the velocity fluctuations depends strongly on the ratio of the forces as expressed by the flow parameter.

Reasons for this behaviour may lie in the nature of natural convection over a horizontal surface. Three regions may be distinguished: the viscous–conductive layer, a transition layer of fully turbulent flow that is strongly influenced by the viscous layer, and a 'similarity' region in which the convection is determined only by the buoyancy flux and by the presence of the surface as a constraint on the motion. Observations in the transition layer (Townsend 1959*b*; Deardorff & Willis 1967) show that temperature fluctuations are strongly intermittent but that velocity fluctuations are continuous, and it is likely that most of the heat is transferred from the viscous layer in the form of 'plumes' or streamers of hot fluid. Unlike isolated buoyant plumes, these plumes emerge from the viscous layer and come into contact with an environment of strongly turbulent, cold fluid whose temperature is nearly uniform compared with the temperature excess of the plume. Consequently, the plumes are eroded as they rise, losing heat to the surrounding fluid and becoming very weak after rising to a height of perhaps ten thicknesses of the viscous layer (see figure 11). Here the measured distributions of mean temperature and temperature fluctuations will depend on the initial properties of the plumes as well as the rate of erosion, and they are unlikely to conform to assumptions of wall similarity. Outside the transition layer, the similarity assumptions may be valid but the total variation of mean temperature is small compared with that in the other parts of the flow.

In mixed convection with non-zero shear stress, the shearing motion favours the occurrence of long eddies with axes aligned with the flow direction, and the plumes ejected from the viscous layer are expected to be nearly two-dimensional in form. Because of their alignment, they will be affected comparatively little by the mean velocity gradients and, as for natural convection, the temperature profiles will depend on the initial properties of the plumes and on their rate of erosion by the surrounding turbulent fluid. The more important properties of the emergent plumes are (i) their average initial width, presumably a set fraction of the thickness of the viscous layer, (ii) their average temperature excess and (iii) their average velocity of ejection. The magnitudes of the last two should be

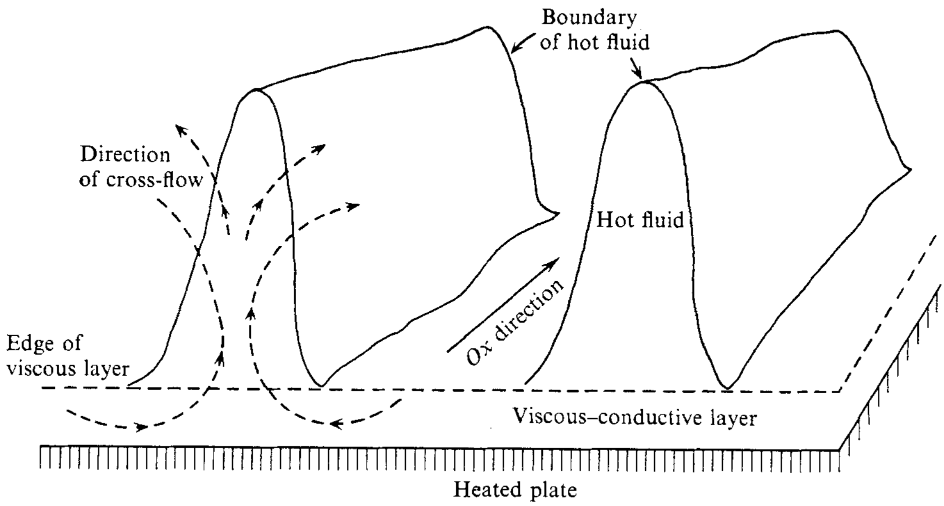

FIGURE 11. Sketch of hot plumes ejected from the viscous layer and undergoing erosion by the cold turbulent fluid surrounding them.

comparable with the root-mean-square fluctuations of temperature and of velocity at the edge of the layer. Now the behaviour of a buoyant plume depends on the ratio of the momentum flux supplied at ejection to that obtained from acceleration by buoyancy forces. If the ejection velocity is u_e and the ejection temperature excess is θ_e, the relative importance of buoyancy forces on the development is measured by the magnitude of the plume Richardson number $g\theta_e z_m/u_e^2$. If u_e and θ_e are identified with the root-mean-square fluctuations, the Richardson number is about 0·15 for natural convection and much less for mixed convection, and it is plausible that the development of the plumes is unaffected by their buoyancy in natural or mixed convection until they rise beyond the region of rapid variation of mean temperature.

We now have plumes of negligible buoyancy (really jets) propagating into and being eroded by turbulent fluid whose velocity fluctuations are comparable with the velocity of emergence, and, since the motion is little affected by viscosity, the distance that they move before undergoing a set amount of erosion is a constant multiple of their initial width and is independent of the flow parameter. Then, in the transition region where the emergent plumes are broken up by the general turbulent motion, the main features of the temperature structure should be the same for all flow parameters, with length and temperature scales which are the scales for the viscous–conductive layer as well.

Although the experimental flows cover much the same range of Richardson numbers as do the observations that have been made of the earth's boundary layer with upward transfer of heat, an essential difference is the absence of a fully turbulent region of forced convection above the viscous and transition layers. In the region of forced convection (approximately for $z/L < 0{\cdot}05$) the temperature distribution is given by

$$\phi_h \equiv \frac{\kappa\tau_0^{\frac{1}{2}} z}{QT}\frac{dT}{dz} = \text{constant} \tag{7.2}$$

and the turbulent motion is composed to a large extent of eddy structures of the twin-vortex form described by Kline, Reynolds, Schraub & Runstadler (1967) and many others. At heights comparable with the Monin–Obukhov length L buoyancy forces will transfer energy to the eddies and tend to elongate them in the vertical direction. If the elongation is sufficient to make them resemble the plumes emerging from the viscous layer, their development as they rise may be geometrically similar and the temperature structure similar to that observed in the laboratory flows. Some confirmation of the surmise can be obtained from the observed intermittency of temperature fluctuations in strongly unstable atmospheric flows and the considerable region in which the temperature distribution follows neither the forced convection form (7.2) nor the similarity form for natural convection,

$$\phi_h = \text{constant} \times (z/L)^{-\frac{1}{3}} \tag{7.3}$$

(see, for example, Dyer 1967). Naturally, the relevant scales of temperature and length are not determined by properties of a probably non-existent viscous layer but by properties of the forced convection flow just below the transition region. That is to say, the length scale should be a fraction of L (possibly about 0·05) and the temperature scale comparable with the 'friction temperature' $Q/\tau_0^{\frac{1}{2}}$.

In the experimental flow for $U_a/u_1 = 25$, the non-dimensional magnitudes of the velocity and temperature fluctuations (based on shear stress and heat flux) are not far from those in atmospheric boundary layers over a similar range of z/L, and the convective flow in its transition region may resemble closely the flow in the transition region between forced and natural convection in an atmospheric layer. If this is so, the measured distribution of mean temperature is broadly consistent with the result of Dyer (1967),

$$\phi_h = (1 + 15z/L)^{-0\cdot 55}. \tag{7.4}$$

Both the atmospheric and the laboratory measurements suggest that the variation of mean temperature in the region of natural convection (say $z/L > 3$) is small compared with that in the transition region.

Appendix. The sea-breeze flow at the entrance to the duct

As the cold air from the blower passes over the heated floor of the duct, it is heated and the horizontal gradients of temperature cause flow accelerations and, particularly for low velocities of flow, velocity profiles with strong maxima about 20 mm above the floor. This effect cannot be avoided without preheating of the air and it constituted a serious obstacle to making measurements in conditions of large negative Richardson number. The sea-breeze effect is also of some interest for its own sake and, although few relevant measurements were made, some discussion of its origin and magnitude may be in order.

Suppose an ideal flow in which air of uniform velocity U_0 and uniform temperature T_0 enters a two-dimensional duct of height $2D$ where it acquires heat by transfer from the floor. If a stream function ψ is used to describe the differences in flow velocity from U_0, the equation for the span-wise component of mean vorticity is

$$(U\partial/\partial x + W\partial/\partial z)\nabla^2\psi = -\frac{g}{T}\frac{\partial T}{\partial x} + \frac{\partial^2 \tau_{13}}{\partial z^2} + \frac{\partial^2}{\partial x\,\partial z}(\tau_{11} - \tau_{33}) - \frac{\partial^2 \tau_{13}}{\partial x^2}. \quad \text{(A 1)}$$

Integrating along a streamline of the mean flow, we find that

$$\overline{U}\nabla^2\psi = -g\frac{T-T_0}{T_0} + \int_{-\infty} \frac{\partial^2 \tau_{13}}{\partial z^2}dx + \frac{\partial}{\partial z}(\tau_{11} - \tau_{33}) - \frac{\partial \tau_{13}}{\partial x}, \quad \text{(A 2)}$$

where $\overline{U}$ is an average velocity along the streamline. If the velocity distribution is changing slowly along the duct, $\nabla^2\psi \approx \partial U/\partial z$ and (A 2) describes the velocity profile if the temperature distribution and the stresses are known.

A first solution may be found by neglecting the friction terms, supposing that the temperature over most of the section is uniform and equal to T_a, and replacing $\overline{U}$ by U_0. Remembering that the continuity condition requires that

$$\int_0^{2D} (U - U_0)\,dz = 0,$$

the required solution is found to be

$$\frac{U-U_0}{U_0} = \frac{g(T_a - T_0)D}{T_0 U_0^2}\left(1 - \frac{z}{D}\right). \quad \text{(A 3)}$$

During runs with small flow velocities, reference temperatures were about 10 °K above the temperature of the inlet air (no systematic measurements were made) and putting $U_0 = 0{\cdot}2\,\mathrm{m\,s^{-1}}$ and $D = 0{\cdot}15\,\mathrm{m}$ in (A 3) leads, for this case, to

$$\frac{U-U_0}{U_0} = 1{\cdot}1\left(1 - \frac{z}{D}\right). \quad \text{(A 4)}$$

Comparison of the solution with the velocity profile at station 4 shown in figure 2 shows that the observed maximum velocity is rather less than the velocity given by (A 4) at the same position and the agreement may appear satisfactory. If some allowance for the difference between $\overline{U}$ and U_0 is made, e.g. by putting $\overline{U} = \frac{1}{2}(U + U_0)$, the indicated velocity is rather less than that observed and it must be concluded either that the net effect of friction is very small or that it acts to accelerate the sea-breeze.

Beyond station 4, Reynolds stresses are sufficient to retard flow near the velocity maximum, accelerations being comparable with the average acceleration from the duct entry to that station, and it is hard to believe that they have had no influence on the flow. If the velocity measurements are believed, the pattern of Reynolds stresses in the early part of the duct must have intensified velocity gradients at a rate comparable with that due to horizontal temperature gradients. Of the stress terms in (A 2), only the first could be comparable with the buoyancy term once convection is established over the whole duct, and it will have the proper sign if $\partial^2\tau_{13}/\partial z^2$ was negative for the greater part of the streamline to the section of observation.

At the duct entrance, a boundary layer of retarded and heated fluid forms on the floor and becomes thermally unstable after its thickness reaches a critical

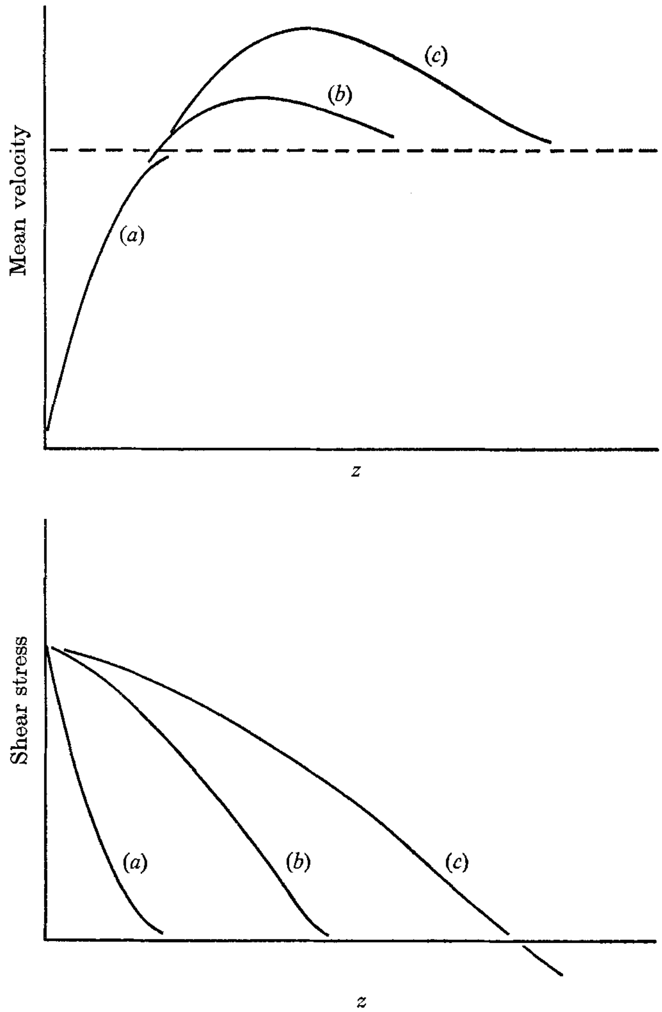

FIGURE 12. Stress and velocity profiles near the entry to the heated duct. (a) Initial stage: no thermal convection outside the shear layer. (b) Later, after thermal convection has transported Reynolds stress out of the shear layer. (c) Still later.

value. Then masses of heated fluid rise from the retarded layer, carrying with them not only heat but also Reynolds stresses generated in the strong shear of the retarded layer. The convective transfer tends to equalize Reynolds stresses and, if it is strong enough, it is possible that the stress at the edge of the retarded layer is little less than the wall stress. In confirmation, the total thickness of the retarded layer at station 4 is about 10 mm after 1 m development, representing a momentum defect very small compared with an estimate of the total wall friction. Over the entrance length of the duct, the extent of convective flow is limited in the upwards direction, and a small gradient of Reynolds stress near the floor means that $\partial^2\tau_{13}/\partial z^2$ is negative for some distance from the retarded layer (see figure 12). At the stage when convection has spread to about twice the height under consideration it is possible that $-\partial^2\tau_{13}/\partial z^2$ might be as large as $\frac{1}{2}\tau_0/z^2$ (for a parabolic variation of stress), and at the velocity maximum, $z = 20\,\text{mm}$, with $\tau_0 = 0{\cdot}008U_0^2$ (see § 6) and $\partial^2\tau_{13}/\partial z^2 = -8\,\text{s}^{-2}$. Supposing the conditions to persist over a length of 0·2 m, the friction term in (A 2) receives a contribution of perhaps $-80\,\text{mm}\,\text{s}^{-2}$, compared with the contribution from buoyancy forces of $-30\,\text{mm}\,\text{s}^{-2}$. It seems at least possible that the upward transport of Reynolds stress from the retarded layer can augment substantially the effect of buoyancy in intensifying the negative velocity gradient near the floor and lead to the production of a sea-breeze considerably stronger than might have been expected.

The suggested mechanism whereby energy may be transferred to the mean flow by interaction between convective turbulent flow and an adjacent layer of strong shear implies that the Reynolds stress and velocity gradient have opposite signs and, if the diffusion terms in the equation for turbulent energy are forgotten, turbulent energy is transformed into mean flow energy in substantial quantity. Unfortunately, no systematic measurements were made near the entrance to the duct, and the intriguing possibility that a mean flow may be driven by turbulent energy must be considered speculative until the entrance flow is studied in more detail.

REFERENCES

Deardorff, J. W. & Willis, G. E. 1967 *J. Fluid Mech.* **28**, 675.

Dyer, A. J. 1967 *Quart. J. Roy. Met. Soc.* **93**, 501.

Kline, S. J., Reynolds, W. C., Schraub, F. A. & Runstadler, P. W. 1967 *J. Fluid Mech.* **30**, 741.

Taylor, R. J. 1958 *J. Sci. Instrum.* **35**, 47.

Thomas, D. B. & Townsend, A. A. 1957 *J. Fluid Mech.* **2**, 473.

Townsend, A. A. 1959*a* *J. Fluid Mech.* **5**, 209.

Townsend, A. A. 1959*b* *J. Fluid Mech.* **6**, 261.